

Evaluation of Methods for Bolus Arrival Time Determination using a Four-dimensional MRA Flow Phantom

Dennis Säring^a, Nils Daniel Forkert^a, Till Illies^b, Jens Fiehler^b, Heinz Handels^a

^aDepartment of Medical Informatics,

^bDepartment of Diagnostic and Interventional Neuroradiology,
University Medical Center Hamburg-Eppendorf

Abstract

In this paper an evaluation of methods determining the bolus arrival time (BAT) using a four-dimensional flow phantom to simulate 4D MR angiography is presented. Spatiotemporal 4D MRA images were acquired for analyzing the hemodynamic characteristics of cerebral vessel anomalies. Model-independent and model-dependent methods for BAT extraction are published. Generally, for the evaluation no gold standard exists and datasets with known BAT values are required. Here, a 4D flow phantom is generated based on a synthetic 3D MRA dataset with BAT values defining the time point of blood inflow for each voxel. Then, voxel-by-voxel concentration-time curves based on the gamma-variate function were computed leading to a simulated 4D MRA dataset. Additionally, partial volume effects and Gaussian noise were integrated. The simulated 4D MRA was visually inspected and regarded as similar to clinical data. Finally, phantom datasets with different vessel diameter and signal-to-noise ratio are computed. Three state-of-the-art methods were used to extract BAT values. Computed and known values were compared. The results suggest that model-dependent approaches perform better than the model-independent method.

Keywords:

Hemodynamics, Blood flow, Vascular disease, Phantoms, Imaging

Introduction

Cerebral vascular diseases like aneurysms or arteriovenous malformations are one of the major causes of death worldwide [1]. For an improved rating of the disease and therapy planning detailed knowledge about the individual vessel anatomy and hemodynamic situation is needed [2].

Generally, imaging techniques like 3D computer tomography (CT) or digital subtraction angiography (DSA) are clinical standard for the analysis of the hemodynamics. Unfortunately, those techniques are based on ionizing radiation. Furthermore Warnock et al. [3] reported that the DSA as an invasive procedure has a complication rate of approx. 3.8% and supplies only

2D projections of the vessel system. Recently, new parallel MR image acquisition techniques enables the time resolved 4D MRA imaging of the blood flow. In clinical practice these spatiotemporal 4D MRA images were acquired for the qualitative and quantitative analysis of hemodynamic characteristics of cerebral vessel anomalies like arteriovenous malformations (AVMs) or aneurism. Figure 1 shows an image sequence of a 4D TREAT MRA dataset from a patient with AVM.

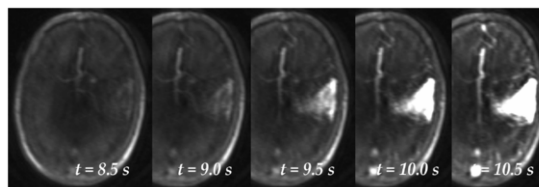


Figure 1- Temporal image sequence of a 4D TREAT MRA

Detailed evaluation of the arterial inflow and venous drainage of AVMs is important for clinical evaluation and management [4,16]. A lot of research has been done on simulation and determination of the cerebral blood flow. In 3D datasets often computational fluid dynamics (CFD) [5] were used to simulate the blood flow. Unfortunately, these approaches are computational expensive and due to acquisition time requirements the vascular system is often not completely covered by the resulting images [8].

In 4D image sequences BAT values can be determined by analyzing the concentration time curves after bolus-injection [6,7]. Here, the tracking of the signal changes provided by an injected bolus of contrast agent travelling through the vessels is used for further analysis. The focus of this work is the evaluation of methods that extract hemodynamic characteristics based on the concentration-time curves of 4D MRA.

State-of-the-art Methods for Determination of Bolus Arrival Time in 4D MRA Image Sequences

The number of publications dealing with determination of the bolus arrival time in 4D MRA is high [8]. Commonly used

approaches for analysis of concentration-time curves can be classified as model-independent or model-dependent.

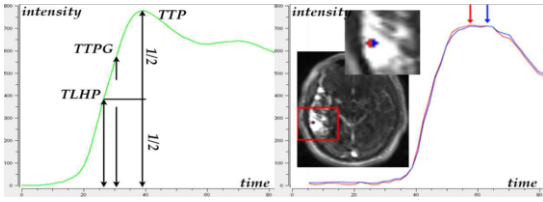


Figure 2- Concentration-time curve with criteria TTP, TTPG and TLHP (left) and the unexpected time difference of two neighbouring vessel voxels using TTP as BAT (right)

Model-independent approaches estimate the BAT directly based on the concentration-time curve. Therefore several criteria have been proposed e.g. time to peak (TTP), time to peak gradient (TTPG) or time of leading half-peak (TLHP) [9]. The major drawback of the model independent criteria is the fixed discrete BAT estimation which depends on the temporal resolution of the used data. Furthermore, it has been reported that due to noise and artefacts e.g. interpolation during the image acquisition these parameters lead to insufficient results, in terms of strong temporal differences between the bolus arrival times of neighbouring voxels [10]. Figure 2 shows the proposed criteria TTP, TTPG and TLHP (left) and the concentration-time curves of two vessel voxels and their temporal difference using TTP as BAT (right).

One *model-dependent* approach is the BAT estimation based on the fit of a gamma variate function

$$C(t) = K(t - AT)^\alpha e^{-(t-AT)/\beta} \quad (1)$$

to the concentration-time curve [10,11]. Eq. 1 is valid for $t > AT$ where t is the independent variable, AT the appearance time, K the constant scale factor and α and β are arbitrary parameters describing the shape. After fitting the gamma variate function to the concentration-time curve the BAT value is determined by extracting one criterion e.g. TTP, TTPG or TLHP of the fitted gamma variate function. Due to the mathematical properties of this function the extracted BAT value is not constrained by the temporal resolution of the given 4D MRA dataset. Unfortunately, the gamma variate fitting can lead to unsatisfying results when applied to concentration-time curves resulting from a rapid injection of a small bolus like in 4D TREAT MRA [12]. Additionally, due to the blood recirculation the realistic concentration-time curves do usually not only consist of the first pass bolus but do also show following bolus passages. So, the concentration-time curve is not as steep as the assumed hypothetical exponential decay [13].

Another *model-dependent* approach was published by Forkert et al. [8]. Here, a patient-individual reference curve $r(t)$ is generated based on a collection of present concentration-time curves $s_i(t)$. Based on $r(t)$ one criterion is e.g. TTP, TTPG or TLHP is used to define the BAT. Estimating a linear transformation $f(x) = Ax + B$ the concentration-time curves of all

vessel voxels were fitted to the reference curve such as $r(t) \approx s_j(f(t))$. The estimated fitting parameter A and B can be used to adapt the extracted criterion to determine the BAT value for the signal curve.

In order to assess the accuracy and precision of the presented methods different approaches were used. In general a qualitative evaluation was done by obtaining clinical datasets from normal volunteers. The results were compared with predicted values based on physiological and anatomical findings [6]. Additionally, series of Monte Carlo simulations were performed using realistic synthetic concentration-time curves with known parameters and covering a range of signal-to-noise ratios (SNR) [14]. As a drawback most studies focused only on the determination of the cerebral blood volume. Also the impact of selecting the optimal criteria, e.g. TTP, TTPG or TLHP for BAT estimation was not investigated.

Aim of this Work

In this paper we evaluate the aforementioned three state-of-the-art approaches with three different BAT criteria and three different pre-processing approaches for determining BAT values in 4D MRA concerning quality and robustness. Therefore, we generate a four-dimensional flow phantom to simulate 4D MRA using an extended version of the established gamma variate function. The quality is assessed by calculating and analyzing the differences between synthetic and extracted BAT values. For the robustness the chosen methods are applied to phantom datasets with different vessel diameter and varying signal-to-noise ratio (SNR). Additionally, we evaluate the optimum criteria for BAT determination.

Materials and Methods

Generation of a 4D MRA Flow Phantom

For generation of a synthetic 4D MRA flow phantom the following steps are applied.

- Extraction of realistic geometric vessel structures based on clinical three-dimensional time-of-flight MRA (3D TOF MRA).
- Generation of a synthetic 3D MRA dataset and definition of bolus-arrival-time for each vessel voxel.
- Simulation of 4D MRA datasets based on the gamma variate function considering the partial volume effects (PVE) and the signal-to-noise ratio (SNR)

These steps are described in detail in the following.

Extraction of Realistic Geometric Vessel Structures

Providing realistic geometric vessel structures a vessel system was segmented based on clinical 3D TOF MRA and a 3D model of a part of the system was generated. Then, a centerline was computed and the vessel bifurcations as well as the endpoints of the branches were detected and organized in a network. The geometrical characteristics of the bifurcations of the 3D vessel model are represented in this network by a parameter set including the position and the diameter. Based on

this information tube structures are used to build a synthetic representation of the original vessel structure. The parameter set e.g. the diameter value for each bifurcation can be adjusted for further evaluation.

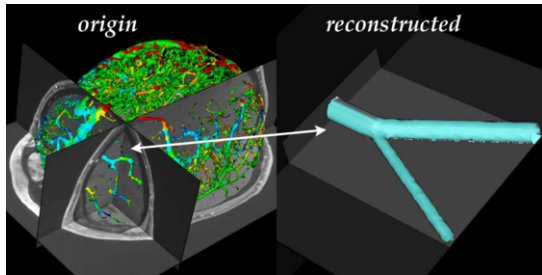


Figure 3- 3D surface model of the original (left) and the reconstructed geometric structure of the vessels (right)

Generation of the 3D MRA and BAT

The generation of a 4D MRA flow phantom dataset requires the definition of bolus arrival times. Therefore, the parameter set was extended by a new BAT entry. Then, the synthetic 3D vessel representation was transferred to a 3D image dataset with high spatial resolution. The image extents and voxels size as well as the intensity values for the vessels, brain structures and background were chosen based on clinical 3D TOF MRA. Additionally, a BAT value was computed for each vessel voxel. Here, a linear interpolation of the BAT of the neighboring bifurcation or end points is used. Figure 3 shows the 3D surface model of the original (left) and the reconstructed geometric structure of the vessels with different diameter (right).

Simulation of 4D MRA

The simulation of spatiotemporal 4D MRA image sequences based on a synthetic 3D MRA dataset requires the simulation of concentration-time curves for each vessel voxel. Therefore, the established gamma variate function (1) is used with $\alpha = 3.0$ and $\beta = 1.5$ regarding to the values published by Chen et al. [15]. In order to address the effect of recirculation of the contrast agent bolus the final concentration-time curve is computed by adding two gamma variate functions with different scaling factors $K_1 = 400$ and $K_2 = 80$ as well as different appearance time points $AT_1 = BAT$ and $AT_2 = BAT + \delta t$ with $\delta t = 8$ frames. Figure 4 shows a clinical concentration-time curve with a fitted gamma variate function (left) as well as a generated signal curve $C(t)$ (right).

Then, a temporal sequence of 3D MRA images is generated where the intensity of each vessel voxel V at time point t_i with $i = 0 \dots n$ are defined by its concentration-time curve $C_V(t_i)$ leading to a 4D MRA with high spatial resolution.

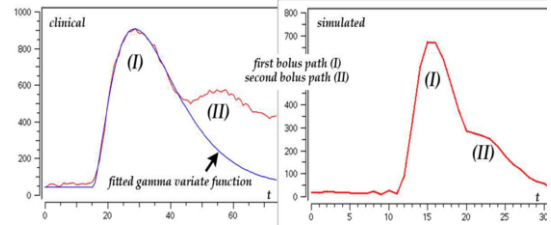


Figure 4- A clinical concentration-time curve with a fitted gamma variate function (left) as well as a generated concentration-time curve (right).

The acquisition of clinical 4D MRA datasets has a tradeoff between temporal and spatial resolution. To improve the temporal resolution the spatial resolution is decreased leading to a partial volume effect (PVE) that can have a significant impact on the accuracy of blood flow measurement [15]. To get realistic synthetic datasets the PVE is simulated by reducing the spatial resolution of the generated 4D MRA as described in [15]. Finally, Gaussian noise with different standard derivation σ is added to simulate the variance of SNR in clinical datasets.

Evaluation Procedure

4D MRA Phantom Datasets

Firstly, the quality of the generated 4D MRA was rated. Therefore, the synthetic image data was visually inspected and compared to clinical image data by two medical experts with experience in 4D MRA image analysis. Related to the clinical datasets the voxel size of the phantom was computed using a spatial resolution of $0.47 \times 0.47 \times 0.5 \text{ mm}^3$ for 3D MRA and $1.88 \times 1.88 \times 4.0 \text{ mm}^3$ with 50 time frames for 4D MRA.

Secondly, different 4D MRA datasets for the evaluation of the BAT determination were generated, one dataset representing four vessels without bifurcation but different diameters ($d = 0.5, 1.0, 2.0 \text{ mm}$) to evaluate the robustness concerning vessel thickness and image artifacts e.g. noise. Another dataset was generated representing a part of a vessel system with one bifurcation and different BAT values for each draining vessel to evaluate the quality concerning different flow characteristics.

Also, each dataset is generated with different signal-to-noise ratio (SNR = 5, 10, 20) to evaluate the quality concerning different noise levels. This leads to 20 synthetic 4D MRA datasets for the evaluation process.

Image Pre-Processing

The model-independent and the model-dependent methods were used to compute the BAT values based on the raw concentration-time curves derived from the generated 4D MRA phantom datasets. Furthermore, since concentration time curves are usually affected by noise and other artifacts, the BAT values were also extracted based on B-Spline approximated (degree of 4) and binomial smoothed (1-4-6-4-1) signal curves in order to investigate whether smoothing is useful to improve robustness.

Similarity Measurement

For quantitative evaluation a regression analysis of the extracted and the defined BAT values of all vessel voxels is computed. Here, the correlation coefficient R^2 is used to quantify goodness of the fit. Whereas, a R^2 value near to one indicates a good fit.

For qualitative evaluation the 3D visualization was used. Here, the extracted BAT values are mapped color-coded on the 3D surface model of the vessel system. Due to the fact that the BAT values in between the bifurcations and endpoints are linear interpolated the color gradient should be homogeneous in case of optimal BAT determination.

Results

Quality of 4D MRA Flow Phantom

The generated 4D MRA image sequences were visually inspected by two medical experts. Therefore, 4D TREAT MRA datasets acquired on a 1.5T MR scanner with SNR between 10 and 25 of 20 patients with known AVM are used to compare. Figure 5 shows the comparison of clinical and simulated 3D and 4D MRA images (left) and the color-coded BAT values (right). The images with SNR = 10 were rated as most similar to the clinical one.

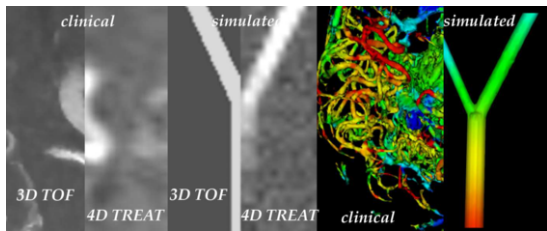


Figure 5- Comparison of clinical and simulated MRA images (left) and its color-coded BAT values (right).

Comparison of the Methods

For comparison of the model-independent (MI), gamma variate fit (GV) and reference based curve fitting (RCF) approaches with three different BAT criteria and three different pre-processing approaches were used to extract BAT values

Table 1 – R^2 values for the BAT determination using different criteria (TTP = 1, TTPG = 2, TLHP = 3) computed based on a phantom dataset with SNR = 10.

	MI			GV			RCF		
	1	2	3	1	2	3	1	2	3
RAW	.985	.960	.967	.932	.971	.986	.991	.981	.987
BIN	.970	.970	.977	.975	.968	.978	.977	.980	.979
SPL	.986	.962	.966	.949	.970	.969	.987	.970	.987

based on the simulated datasets with bifurcation. Table 1 shows the results of the regression analysis (R^2) using different criteria based on the phantom dataset with SNR = 10.

Figure 6 shows the regression analysis of MI, GV and RCF using the THLP criteria and the RAW pre-processing (left). The model-independent approach depends on the discrete time points which leads to a step function line representation of the BAT times ($R^2 = 0.967$). The results in Figure 6 (right) show that the model-dependent methods have the best fit. Generally, the combination of reference-based curve-fitting, RAW pre-processing and the TLHP or TTP criterion leads to the highest accuracy.

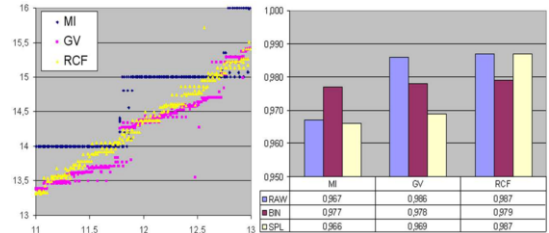


Figure 6- Regression analysis of MI, GV and RCF using the THLP criteria based on the RAW signal curves (left) and the calculated R^2 values for the approaches using THLP (right).

Influence of SNR

For evaluation of the influence of SNR the simulated datasets with tubes generated with different diameters and disturbed by Gaussian noise were used. Figure 7 shows the R^2 values of the regression analysis for MI, GV and RCF using THLP based on a tube structure with $d = 1mm$. The results show the quality and the robustness of the RCF approach concerning image artifacts in comparison to the other approaches. For SNR = 5 and $d > 2 mm$ the R^2 values of all methods get similar. But, with vessel structures of $d = 0.5 mm$ the value for the MI approach decreased to 0.929 (GV = 0.996 and RCF = 0.998).

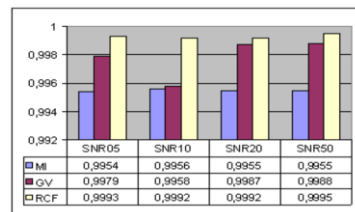


Figure 7- R^2 values of the regression analysis for MI, GV and RCF using THLP based on a tube structure with $d = 1mm$.

Discussion

We have evaluated three methods for BAT determination based on a 4D MRA flow phantom. Based on the gamma variate function for each vessel voxel a realistic concentration-time curve including the recirculation effect was generated. In a post-process these curves were disturbed by Gaussian noise

and partial volume simulation. The synthetic 4D MRA datasets were rated as similar to clinical 4D MRA by two medical experts.

For the evaluation process a number of 4D MRA datasets were generated with varying parameters like SNR or vessel diameter. The voxel-by-voxel definition of the BAT values enables the validation of BAT determination methods concerning robustness and accuracy. Three state-of-the-art approaches with different BAT criteria and different pre-processing were evaluated based on the 4D flow phantom. The results show that the model-dependent methods have the best potential for extraction of hemodynamic characteristics. In particular the reference-based curve-fitting obtains the most accurate results.

Due to the fact that the gamma variate function is used to generate the concentration time curves the best result was expected to be based on the GV approach. Nevertheless, the simulation of the second bolus and the image artifacts leads to a realistic modified signal curve enabling the evaluation of different methods for BAT determination.

In future the accuracy of the 4D flow phantom concerning physiological aspects should be improved by integrating e.g. poiseuille flow conditions to simulate the dispersion of a bolus during a flow down a tube. Furthermore, the recirculation process should be extended by varying the peak of first and second bolus regarding to the vessel diameter. For the evaluation process more parameters describing hemodynamic characteristics like cerebral blood volume, cerebral blood flow and mean transit time should be integrated.

Acknowledgments

This work is supported by German Research Foundation (DFG, HA 2355/10-1).

References

- [1] Donnan, GA, Fisher M, Macleod M, and Davis SM. "Stroke". *The Lancet* 2008; 371:1612-1623.
- [2] Choi, J and Mohr J. Brain arteriovenous malformations in adults. *Lancet Neurol* 2005; 4:299-308.
- [3] Warnock N, Gandhi M, Bergvall U, and Powell T. Complications of intra arterial digital subtraction angiography in patients investigated for cerebral vascular disease. *Brit J Radiol* 1993; 66:855-858.
- [4] Ledezma CJ, Hoh BL, Carter BS. Complications of cerebral arteriovenous malformation embolization: multivariate analysis of predictive factors. *Neurosurgery* 2006; 58:602-11
- [5] Jialiang C, Shengzhang W, Wei Y, and Guanghong, D. Computational fluid dynamics modeling of intracranial aneurysms. *International Conference on BioMedical Engineering and Informatics* 2008; 566-569.
- [6] Østergaard L, Weisskoff RM, Chesler DA, Gyldensted C, Rosen BR. High resolution measurement of cerebral blood flow using intravascular tracer bolus passages. I. Mathe-

tical approach and statistical analysis. *Magn Reson Med* 1996; 36:715-725.

- [7] Østergaard L, Sorensen AG, Kwong KK, Weisskoff RM, Gyldensted C, Rosen BR. High resolution measurement of cerebral blood flow using intravascular tracer bolus passages. II. Experimental comparison and preliminary results. *Magn Reson Med* 1996; 36:726-736.
- [8] Forkert ND, Säring D, Fiehler J, Illies J, Möller D, Handels H. Analysis and Dynamic 3D Visualization of Cerebral Blood Flow Combining 3D and 4D MR Image Sequences. In: Miga MI, Wong KH, eds. *Visualization, Image Guided Procedures, and Modeling*, SPIE Medical Imaging 2009; 7261:331-338.
- [9] Shpilfoygel SD, Close RA, Valentino DJ and Duckwiler GR. X-ray videodensitometric methods for blood flow and velocity measurement: A critical review of literature. *Med Phys* 2000; 27(9): 2008-2023.
- [10]Thompson HK, Starmer CF, Whalen RE and McIntosh HD. Indicator transit time considered as a gamma variate. *Circ Res* 1964; 14:502-515.
- [11]Madsen MT. A simplified formulation of the gamma variate function," *Phys Med Biol* 1992; 37(7): 1597-1600.
- [12]Cunningham I, Hobbs B and Fenster A. A new system for quantitative arterial imaging and blood flow measurements. *Invest Radiol* 1986; 21(6):465-71.
- [13]Benner T, Heiland S, Erb G, Forsting M, Sartor K. Accuracy of gamma-variate fits to concentration-time curves from dynamic susceptibility-contrast enhanced MRI: influence of time resolution, maximal signal drop and signal-to-noise. *Magn Reson Imaging* 1997;15(3):307-17.
- [14]Perkiö J, Aronen HJ, Kangasmäki A, Liu Y, Karonen J, Savolainen S, Østergaard L. Evaluation of four postprocessing methods for determination of cerebral blood volume and mean transit time by dynamic susceptibility contrast imaging. *Magn Reson Med* 2002; 47(5):973-81.
- [15]Chen JJ, Smith MR, Frayne R. The impact of partial-volume effects in dynamic susceptibility contrast magnetic resonance perfusion imaging. *Magn Reson Imaging* 2005; 22(3):390-399
- [16]Säring D, Fiehler J, Forkert ND, Piening M and Handels H. Visualization and analysis of cerebral arteriovenous malformation combining 3D and 4D MR image sequences. *International Journal of CARS* 2007; 2:75-79.

Address for correspondence

Dr. Dennis Säring
Department of Medical Informatics
University Medical Center Hamburg-Eppendorf
d.saering@uke.uni-hamburg.de